Mechanics & Industry **20**, 102 (2019)

https://doi.org/10.1051/meca/2018051

Mechanics & Industry

Available online at:
www.mechanics-industry.org

Regular Article

Fault detection of damper in railway vehicle suspension based on the cross-correlation analysis of bogie accelerations

Mădălina Dumitriu*

Department of Railway Vehicles, University Politehnica of Bucharest, 313 Splaiul Independenţei, 060042 Bucharest, Romania

Received: 31 August 2018 / Accepted: 24 November 2018

Abstract. Nowadays, the condition-based maintenance is associated more and more with railway transport to improve the safety, availability, reliability and capacity of this transport system, and to reduce life cycle costs for the railway vehicles. The condition-based maintenance requires that vehicle components are replaced based on their real condition, which implies the fault detection and isolation during the train's operation. The paper proposes a method to detect the failure of the damper in the primary suspension of the rail vehicle, based on the analysis of cross-correlation of the vertical accelerations measured on the bogie frame against the two axles. The numerical simulations and experimental results show a very good correlation between the bogie accelerations when the dampers are in a normal operation condition. This thing is shown based on the values of the cross-correlation coefficient (CCC) of the bogie accelerations. The failure in a damper can be detected by the decrease of the CCC of the bogie accelerations, a confirmed fact in the results derived from numerical simulations. The proposed method has more advantages, namely, it is a signal-based method and hence does not require a complex mathematical modelling of the vehicle-track system and knowledge of its parameters or of the external conditions; the method makes relative comparisons between measurements and hence reduces the effect of the factors that influence outputs; the method can be also extended for the secondary suspension; the method can be easily implemented on any type of bogie.

Keywords: Railway vehicle / primary suspension / cross-correlation analysis / fault detection

1 Introduction

Rail transport must always have the best solutions to match the increasingly demanding requirements of a society in a permanent evolution, where the mobility standards continue to rise. To turn the rail transport into a competitive system, the railroad operators are invariably concerned with providing the availability and punctuality of the transport services, as well as their safety. Basically, avoidance of the unplanned interruptions and the minimization of the vehicle downtime for conducting the activities specific to maintenance should be well considered.

The calendar-based maintenance activities of the rail vehicles take place regularly, and the maintenance intervals are functions of time or mileage. The selection of such intervals relies on theoretical considerations, but mostly on experience, which can lead to much shorter maintenance intervals. A solution to keep the vehicle downtime at a minimum is condition-based maintenance. Unlike the calendar-based maintenance, where the vehicle components are replaced after certain pre-set intervals, the condition-based maintenance implies the replacement based on their real condition, which requires the fault detection and isolation (FDI) occurring during the operation [1]. The technique to analyse the dynamic behaviour of a vehicle during operation is known as condition monitoring, mainly applicable to systems that deteriorate in time, and is aimed at detecting and identifying fault before it causes a failure. This is a key element of the condition-based maintenance [2–4].

The condition monitoring gives a series of benefits to the rail operators. When defects in the operation of the vehicle components are detected in an early stage, the further deterioration in its performance is prevented and safety increased. Repairs or timely replacement of the faulty components increases the reliability and availability of the railway vehicle. Last but not least, the costs associated with vehicle maintenance can be greatly reduced by using the condition-based instead of the calendar-based maintenance.

The reliability of the suspension system of the railway vehicles is essential, on the one hand, for meeting the ride quality and ride comfort and, on the other hand, for

* e-mail: madalinadumitriu@yahoo.com

compliance with the conditions imposed by the traffic safety [5–8]. The suspension damage generally leads to decrease or increase of the nominal parameters' values – damping and stiffness coefficients. Any deviation from nominal characteristics of suspension influences the dynamic behaviour of the vehicle or, in extreme cases, it can jeopardize the security of passengers. Detecting component faults at their early stages prevents further deterioration in vehicle performance and enhances safety. The rapid and effective monitoring techniques are essential to increase vehicle reliability and reduce maintenance cost [9,10].

The FDI methods in the literature of review fall into two major categories: signal-based methods and model-based methods [2,3]. Mostly, only the output signals can be measured, in which case signal-based methods can be applied. The measured signal is analysed in time and/or frequency domain to find features or signatures related to particular faults. The bandpass filters, spectral analysis, maximum-entropy estimation and wavelet analysis are all applicable as the signal processing method [4]. If the relation between input signal and output signal is available, detection of abrupt faults can be possible, using the model-based fault detection method, through the evaluation of residuals [11–13]. The model-based FDI is mainly divided into the following methods: parameter estimation method, parity equation method and observer/Kalman filter-based method [2].

The paper shows that a method for detecting a damper fault in the primary suspension of the railway vehicle can be based on the cross-correlation analysis of the measured vertical accelerations of bogie. In fact, the method is based on the modification of the cross-correlation coefficient of the acceleration in the bogie frame against the axles during the failure of a damper. This situation is made clear in the results from the numerical simulations based on a bogie-track six-degree of freedom system model, which takes into account the vibration rigid modes of a two-axle bogie – bounce and pitch, the vertical displacement of the wheels and rails and the elasticity of the wheel–rail contact. The failure of the damper is simulated by various degrees of reduction of the damping constant of the suspension corresponding to one of the wheels, compared with the reference value. Basically, a very good correlation between the bogie accelerations calculated against the axles, corresponding to the time delay between the two axles (bogie wheelbase–velocity ratio), means no damper defect. When one of the dampers is faulty, the bogie accelerations are slightly correlated, confirmed by the decrease of CCC of the bogie accelerations. The results on the CCC of the measured accelerations on a bogie in a passenger rail vehicle during travelling on the current line are introduced and they are in agreement with the results from the numerical simulations. To increase the sensitivity and accuracy of the method, the measured accelerations are filtered within the range of the resonance frequencies of bounce and pitch in the bogie by applying a bandpass filter. In this interval, the response of the system is maximum and the most responsive to the change in damping [14].

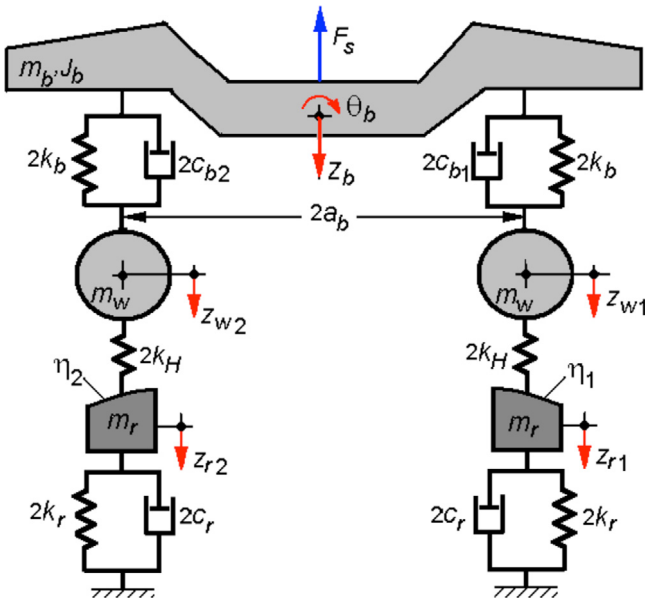

Fig. 1. The mechanical model of the bogie-track system.

The advantage of the suggested method firstly comes from the fact that it is a signal-based method and hence it does not require, as in the model-based methods, a complex mathematical modelling of the system and knowledge of its parameters or of the external conditions (e.g. track input) [15–18], thus providing extra benefits of robustness against nonlinearities and parameter uncertainties. The only parameters of interest are the bogie speed and wheelbase, necessary for calculating the delay in the bogie response against the two suspensions.

In comparison to other signal-based methods that use the absolute signals directly obtained by measuring the accelerations which are depending on the operating conditions [1,9,19,20], the cross-correlation method makes relative comparisons between measurements and hence reduces the effect of the factors that influence outputs.

Even though this method is applied here for the fault detection in the vertical primary suspension, it can be also extended for the lateral primary suspension or for the monitoring of the secondary suspension (vertical or lateral). As for the system of measuring accelerations, this is independent of the bogie configuration and parameters and, therefore, it can be easily implemented on any type of bogie.

2 Analysis of the cross-correlation in the bogie accelerations from numerical simulations

2.1 The mechanical model of the bogie and the motion equations

Figure 1 features the mechanical model of a two-axle bogie travelling at a constant velocity V on a straight track with vertical irregularities. The model of the bogie includes three rigid bodies modelling the bogie frame and the two

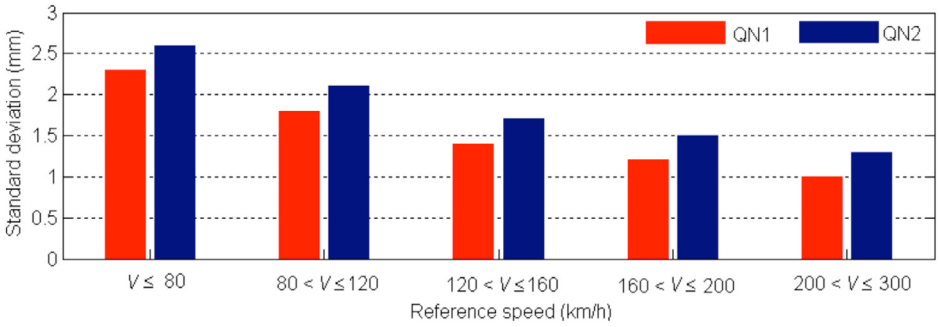

Fig. 2. Standard deviation for vertical alignment for track quality levels QN1 and QN2.

axles connected between them by Kelvin–Voigt-type systems that model the suspension corresponding to each axle. The elastic element of the wheelset suspension has the constant $2k_b$ and the damping elements have the constant $2c_{b1}$ and $2c_{b2}$, respectively. It is assumed that when there is no damper defect, the damping constants of the suspension in the two axles are equal ($2c_{b1} = 2c_{b2}$).

The rigid vibration modes of the bogie in the vertical plane, namely, bounce (z_b) and pitch (θ_b), are taken into account. The bogie parameters are m_b – bogie mass; $2a_b$ – bogie wheelbase; $J_b = m_b i_b^2$ – inertia moment; and i_b – the gyration radius of the bogie. The wheelsets of mass m_w have a translation motion in the vertical direction ($z_{w1,2}$).

Neglecting the coupling effects between the wheels due to the propagation of the bending wavelength, in the frequency domain specific to the vertical vibrations of the vehicle, an equivalent model with lumped parameters will be selected. Against each axle, the track is represented as an oscillating system with one degree of freedom that has a vertical motion, with the displacement $z_{r1,2}$. The equivalent model of the track has mass m_r, stiffness $2k_r$ and the damping coefficient $2c_r$.

The elasticity of the wheel–rail contact will be chosen by introducing certain elastic elements with a linear characteristic. The calculation of the stiffness in the contact elastic elements – $2k_H$ for a wheel–rail pair – is done based on the Hertz's theory of contact between two elastic bodies by applying the linearization of the relation of contact deformation against the deformation corresponding to the static load on the wheel.

The track vertical irregularities are described against each axle via a pseudo-stochastic function [21]:

$$\eta_{1,2}(x_{1,2}) = K_\eta f(x_{1,2}) \sum_{k=0}^{N} U_k \cos\left(\Omega_k x_{1,2} + \varphi_k\right), \text{for } x_{1,2} > 0, \tag{1}$$

with $x_1 = Vt$ and $x_2 = Vt - 2a_b$.

The amplitude U_k of the spectral component, k', corresponding to the wavelength Ω_k, is established with the help of the power spectral density of the track vertical irregularities, as defined in ORE B176 [22]:

$$\Phi(\Omega) = \frac{A_{\text{QN1,2}}\Omega_c^2}{(\Omega^2 + \Omega_r^2)(\Omega^2 + \Omega_c^2)}, \tag{2}$$

where $\Omega_c = 0.8246$ rad/m, $\Omega_r = 0.0206$ rad/m and $A_{\text{QN1,2}}$ is a constant depending on the track quality; for the lag of the spectral component φ_k of the spectral component, $k,'$ an uniform random distribution is selected.

The constant $A_{\text{QN1,2}}$ is calculated so that the standard deviation of the vertical alignment ($\sigma_{\eta\text{QN1,2}}$) due to the components with the wavelength ranging from $\Lambda_1 = 3$ m to $\Lambda_2 = 25$ m correspond with the information in the UIC 518 Leaflet [23], subject to the track quality level, QN1 or QN2 (see Fig. 2)

$$A_{\text{QN1,2}} = 2\pi \frac{\sigma^2_{\eta\text{QN1,2}}}{\Omega_c^2 I_0}, \tag{3}$$

with

$$I_0 = \int_{\Omega_2}^{\Omega_1} \frac{\mathrm{d}\Omega}{(\Omega^2 + \Omega_r^2)(\Omega^2 + \Omega_c^2)}, \quad \text{for } \Omega_{1,2} = 2\pi/\Lambda_{1,2}. \tag{4}$$

The coefficient K_η is a scaling coefficient of the amplitudes in the track vertical irregularities, a result of the ratio between the magnitude of the admitted isolated defect $\eta_{\text{admQN1,2}}$ as in the UIC 518 Leaflet (see Fig. 3) and the absolute magnitude of the vertical irregularities ($\max|\eta(x_{1,2})|$)

$$K_\eta = \frac{\eta_{\text{admQN1,2}}}{\max\left| f(x_{1,2}) \sum_{k=0}^{N} U_k \cos\left(\Omega_k x_{1,2} + \varphi_k\right) \right|}. \tag{5}$$

Function $f(x_{1,2})$ is an adjustment function applied to the distance L_0, in the form of

$$f(x_{1,2}) = \left[6\left(\frac{x_{1,2}}{L_0}\right)^5 - 15\left(\frac{x_{1,2}}{L_0}\right)^4 + 10\left(\frac{x_{1,2}}{L_0}\right)^3 \right] H(L_0 - x_{1,2}) + H(x_{1,2} - L_0), \tag{6}$$

where $H(.)$ is Heaviside step function.

The vertical motions of the bogie-track system are described by six motion equations, corresponding to the vibration modes of the bogie – bounce and pitch, the vertical displacements of the wheels and of the rails.

The equations defining the bounce and pitch motions of the bogies are

$$m_b \ddot{z}_b = \sum_{i=1}^{2} F_{bi} - F_s, \tag{7}$$

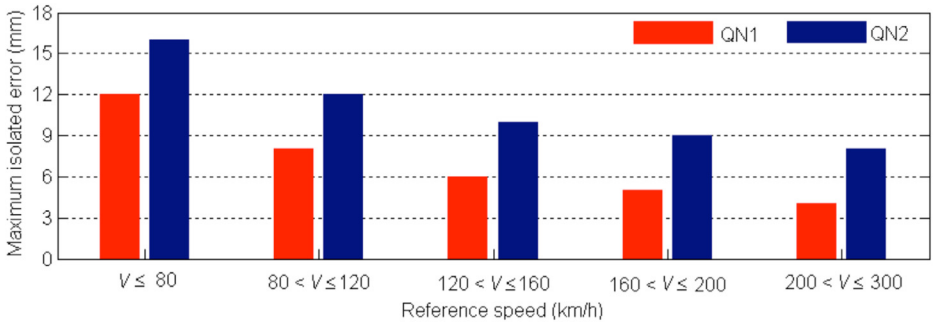

Fig. 3. The peak value for vertical alignment for track quality levels QN1 and QN2.

$$J_b\,\ddot{\theta}_b = a_b\sum_{i=1}^{2}(-1)^{i+1}F_{bi}, \tag{8}$$

where F_s represents the force due to the secondary suspension of the vehicle and F_{bi} are the forces from the primary suspension of the axles i,

$$F_{b1,2} = -2c_b(\dot{z}_b \pm a_b\dot{\theta}_b - \dot{z}_{w1,2}) - 2k_b(z_b \pm a_b\theta_b - z_{w1,2}). \tag{9}$$

The equations of the motions on the vertical direction of each axle are

$$m_w\,\ddot{z}_{w1,2} = 2Q_{d1,2} - F_{b1,2}, \tag{10}$$

where $Q_{d1,2}$ are the dynamic contact forces; the dynamic contact forces on the wheels of an axle are considered to be equal.

To calculate the dynamic forces, the hypothesis of the Hertzian linear contact between the wheel and the rail has been adopted for

$$Q_{d1,2} = -k_H[z_{w1,2} - z_{r1,2} - \eta_{1,2}], \tag{11}$$

where k_{H} is the stiffness of the wheel–rail contact.

The vertical displacements of the rails are to be found in

$$m_w\,\ddot{z}_{r1,2} = F_{r1,2} - 2Q_{d1,2}, \tag{12}$$

where

$$F_{r1,2} = -2c_r\dot{z}_{r1,2} - 2k_r z_{r1,2}. \tag{13}$$

The equations of motion for the bogie-track system become

$$m_b\,\ddot{z}_b + 2c_{b1}(\dot{z}_b + a_b\dot{\theta}_b - \dot{z}_{w1}) + 2c_{b2}(\dot{z}_b - a_b\dot{\theta}_b - \dot{z}_{w2}) + 2k_b[2z_b - (z_{w1} + z_{w2})] - F_s = 0 \tag{14}$$

$$J_b\,\ddot{\theta}_b + 2c_{b1}a_b(a_b\dot{\theta}_b + \dot{z}_b - \dot{z}_{w1}) + 2c_{b2}a_b(a_b\dot{\theta}_b - \dot{z}_b + \dot{z}_{w2}) + 2k_b a_b[2a_b\theta_b - (z_{w1} - z_{w2})] = 0 \tag{15}$$

$$m_w\,\ddot{z}_{w1,2} + 2c_{b1,2}(\dot{z}_{w1,2} - \dot{z}_b \mp a_b\dot{\theta}_b) + 2k_b(z_{w1,2} - z_b \mp a_b\theta_b) + 2k_H(z_{w1,2} - z_{r1,2} - \eta_{1,2}) = 0 \tag{16}$$

$$m_r\,\ddot{z}_{r1,2} + 2c_r\dot{z}_{r1,2} + 2k_s z_{r1,2} + 2k_H(z_{r1,2} - z_{w1,2} + \eta_{1,2}) = 0. \tag{17}$$

A system of six differential equations of second order was thus obtained, in which the variables of state, displacements and velocities are introduced,

$$q_{2k-1} = p_k,\ \ q_{2k} = p_k,\ \ \text{for}\, k = 1\ldots 6, \tag{18}$$

where $p_1 = z_b$, $p_2 = \theta_b$, $p_{3,4} = z_{w1,2}$, $p_{5,6} = z_{r1,2}$. The result will be a system of 12 differential equations of first order that can be written in a matrix-like form:

$$\dot{\mathbf{q}} = \mathbf{A}\mathbf{q} + \mathbf{B}, \tag{19}$$

where $\mathbf{q}$ is the vector of the state variables, $\mathbf{A}$ is the matrix of the system and $\mathbf{B}$ is the vector of the non-homogeneous terms. The system of equations (19) can be solved through a numeric integration by applying the Runge–Kutta algorithm.

2.2 The cross-correlation function of the bogie accelerations

Considering the accelerations of the bogie as stationary and ergodic stochastic processes, the cross-correlation function can be defined in the following form:

$$R(\tau) = \lim_{T\to\infty}\frac{1}{T}\int_{-T/2}^{T/2} a_{b1}(t+\tau)a_{b2}(t), \tag{20}$$

where $a_{b1}(t)$ and $a_{b2}(t)$ are the accelerations of the bogie frame against the axle 1 and the axle 2, respectively, and τ is the delay time between the two accelerations; τ represents the arguments of the cross-correlation function of the accelerations. Further, this τ can range between $-\infty$ and $+\infty$.

The cross-correlation function of the bogie frame accelerations is the measure of the similarity or interdependence between the two accelerations. In practice, this function shows to what extent the acceleration $a_{b1}(t)$ is similar to the acceleration $a_{b2}(t)$ after a certain time interval τ, when this has become $a_{b1}(t+\tau)$. For the numerical simulations or the experiments, there is only a limited sequence of the two accelerations between $t_{\min}$ and $t_{\max}$, with the duration $T_0 = t_{\max} - t_{\min}$. In this case, the

cross-correlation function depends on the time t_0 at which is calculated

$$R(t_0,\tau)=\frac{1}{T}\int_{t_0-T/2}^{t_0+T/2}a_{b1}(t+\tau)a_{b2}(t). \quad (21)$$

For evident reasons, the following condition has to be met:

$$t_{\min}\le t_0-\frac{T}{2}-\tau_{\min},\quad t_0+\frac{T}{2}+\tau_{\max}\le t_{\max}, \quad (22)$$

where $\tau_{\min}$ is the minimum value of τ, while $\tau_{\max}$ is the maximum value.

The cross-correlation function can be noticed to be dependent on the amplitude of the two accelerations. This aspect might represent a major inconvenience herein, since the track quality determines the response of the bogie. For this reason, the CCC of the two accelerations will be used:

$$C_{12}(t_0,\tau)=\frac{R(t_0,\tau)}{\sigma_{a1}\sigma_{a2}}, \quad (23)$$

where σ_{a1} and σ_{a2} are the standard deviations of the accelerations a_{b1} and a_{b2}.

The CCC can take values between −1 and 1, where the highest value means that the two accelerations are perfectly correlated, while the value zero shows the lack of correlation between these accelerations. When the CCC takes the lowest value (–1), the two accelerations show contrary tendencies. A CCC close to 1 confirms the good correlation between the two accelerations.

2.3 The results of the numerical simulations

This section features the results of the numerical simulations regarding the root mean square of accelerations (RMS accelerations) and CCC of the bogie accelerations when running at a constant speed on a track with vertical irregularities.

The parameters of the numerical model were provided for Minden-Deutz bogie (see Tab. 1), while the contribution of 300 spectral components with wavelengths between 3 and 120 m was considered to synthesize the vertical irregularities in the track. The limit values of the interval of the wavelengths were thus calculated so that they are representative for the frequency interval of the bogie vertical vibrations.

The track vertical irregularities were synthesized for a 2000 m distance, for a QN2 quality track (Fig. 4). The standard deviations for the vertical alignment and the peak values of the isolated defects were chosen for the maximum velocity of 140 km/h, namely, $\sigma_{\eta\mathrm{QN2}}=1.7$ mm and $\eta_{\mathrm{admQN2}}=10$ mm (Figs. 2 and 3).

Figure 5a features the RMS accelerations of the bogie frame against the two axles at different velocities, including the maximum velocity of the bogie (140 km/h). The vertical vibrations of the bogie are noticed to amplify due to an increase in the velocity. For instance, a rise in the velocity from 50 to 140 km/h results into a 6-fold value for the RMS acceleration above axle 1 and 10-fold for the same acceleration above axle 2. Similarly, the bogie response is visibly not symmetrical above the two axles, due to the suspension damping and the geometric filtering effect from the bogie wheelbase [24]. The difference between the RMS accelerations in the bogie calculated above the two axles can reach almost 90%, as shown in Figure 5b.

Table 1. The parameters of the numerical model.

Bogie mass	$m_b=2400$ kg
Wheelset mass	$m_w=1400$ kg
Rail mass (under the axle)	$m_r=175$ kg
Bogie wheelbase	$2a_b=2.5$ m
Inertia moment	$J_b=2.28\times10^3$ kg m^2
Elastic constant of the suspension corresponding to a wheel	$k_{\mathrm{zb}}=0.616$ MN/m
Damping constant of the suspension corresponding to a wheel	$c_b=9.05$ kNs/m
Track vertical stiffness	$k_r=70$ MN/m
Vertical damping of the track	$c_r=60$ kNs/m
Stiffness of the wheel–rail contact	$k_{\mathrm{H}}=1500$ MN/m
Force due to the secondary suspension	$F_s=167$ kN

Figures 6a and b show the RMS bogie acceleration above the two axles at a velocity of 137 km/h, calculated for different degrees of failure of a damper in the suspension of an axle. The failure of the damper is simulated by reducing the damping constant by 10–90%. The increase of the bogie acceleration during the failure of a damper in the suspension of an axle is thus underlined. For instance, a reduction in the damping constant by 50% in the suspension of the axle 1 leads to an increased RMS bogie acceleration by 15.2% above axle 1 and by 14.7% above axle 2. If the damping constant in the suspension of axle 2 is lowered by 50%, the RMS bogie acceleration increases by 10.6% above axle 1 and by 19.1% above axle 2.

Figure 7 shows the CCC of the bogie at the velocities of 117 and 137 km/h for three values of the time t_0: 6, 10 and 14 s. Three situations regarding the condition of the dampers have been taken into account: no defect damper ($c_{b1}=c_{b2}=c_b$); defect damper in the suspension of axle 1 ($c_{b1}=0.1\cdot c_b$ and $c_{b2}=c_b$); defect damper in the suspension of axle 2 ($c_{b2}=0.1\cdot c_b$ and $c_{b1}=c_b$). The diagrams exhibit the delay time between the two accelerations, namely, $\tau=-0.077$ s for $V=117$ km/h and $\tau=-0.065$ s for $V=137$ km/h. When there is no damper defect, the maximum value of CCC is observed to be in the immediate vicinity of τ, which shows a very good correlation between the two accelerations. When one of the dampers fails, the CCC has a significant decrease at the τ time. Moreover, the maximum value of CCC is recorded at times different from τ (see Figs. 7a′ and b′).

Figure 8 shows the CCC calculated at $\tau=-2a_b/V$ for $6\,\mathrm{s}\le t_0\le 14\,\mathrm{s}$, while considering different failure degrees of the dampers in the suspension of the front and the axle 2. Where there is no failed damper, the average value of CCC

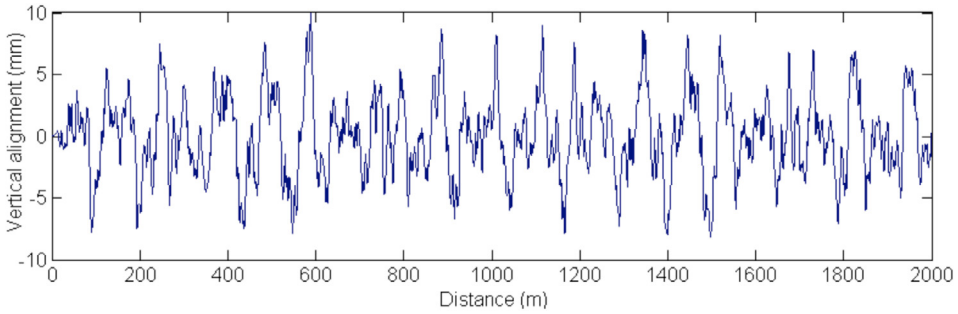

Fig. 4. The vertical track irregularities synthesis.

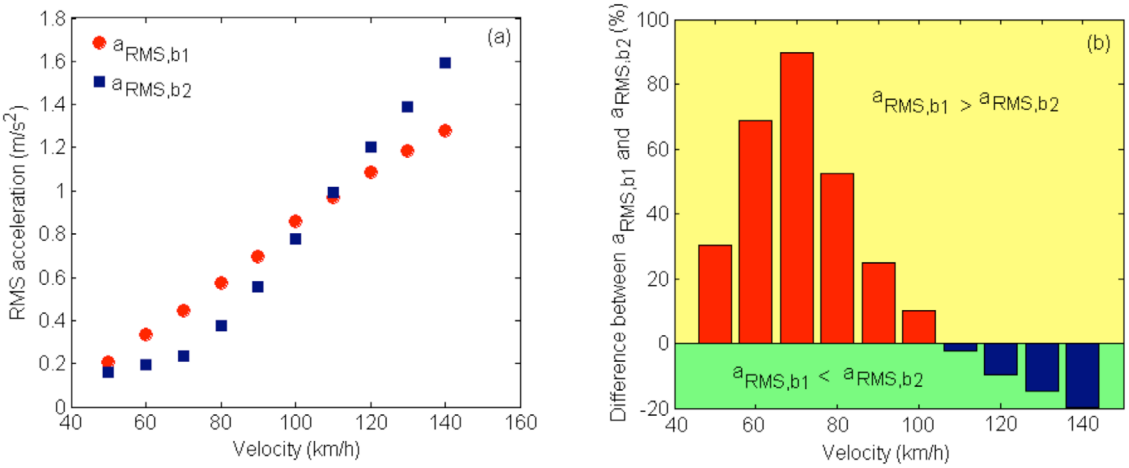

Fig. 5. The RMS velocity-dependent accelerations of the bogie.

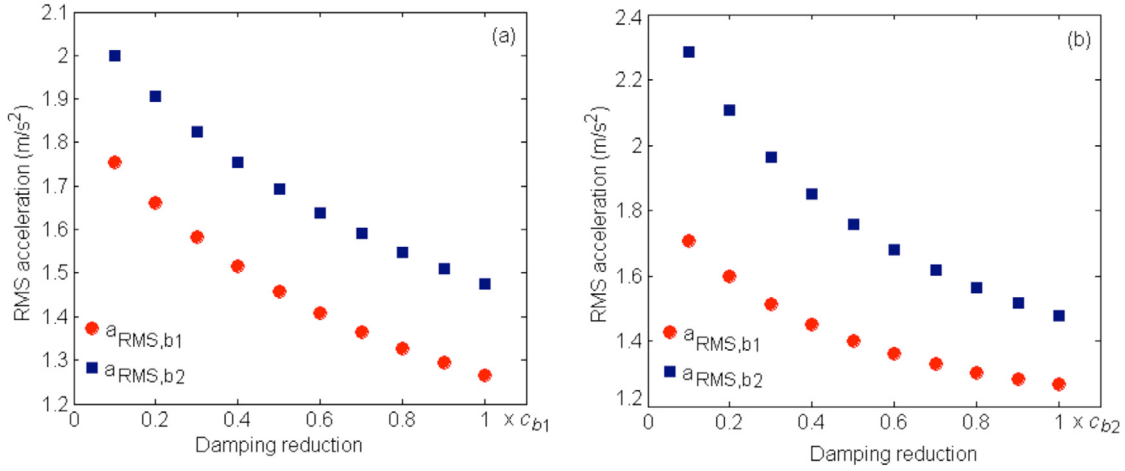

Fig. 6. The RMS acceleration for different degrees of failure in a damper: (a) in the suspension of axle 1; (b) in the suspension of axle 2.

is 0.925, for the circulation at velocity of 117 and 137 km/h. The higher the failure degree of the damper, the lower the value of CCC, which is visible in the average values of CCC in Table 2.

As can be seen, the so-called *area of failure* shown in Figure 8, is limited by the lowest value of CCC of the accelerations calculated for the normal operation state of the dampers. If the values of CCC of the bogie accelerations against the two axles are to be found in this area, it is about a failure of one of the dampers in the suspension of the axles.

The derived results constitute favourable premises for the identification during operation of the failure of dampers in the bogie suspension, based on the CCC of the accelerations measured on the bogie frame against the two axles.

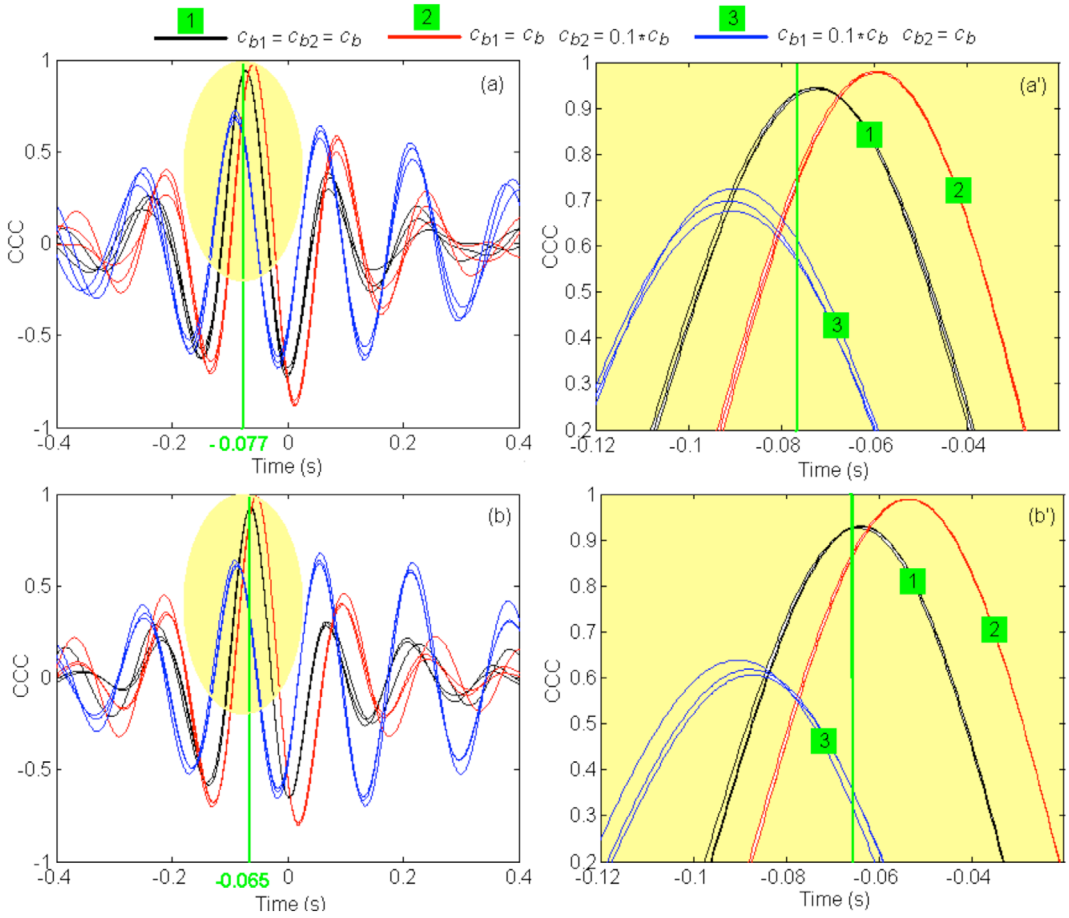

Fig. 7. The CCC of the bogie accelerations: (a) and (a′): at velocity of 117 km/h; (b) and (b′): at velocity of 137 km/h.

3 Analysis of the cross-correlation of the measured accelerations

3.1 Measurement of the bogie accelerations

This section presents the vertical accelerations measured on a Minden–Deutz bogie frame that is fitted on a passenger vehicle for long and medium traffic where the maximum velocity is 140 km/h. Two accelerometers were installed on a side of the bogie, with one accelerometer on the bogie frame against each axle (see Fig. 9).

The measurements were carried out using a measuring chain incorporating, on the one hand, the components of the measurement, acquisition and processing system for the vertical accelerations – namely, four of 4514 Brüel & Kjær piezoelectric accelerometers and the set of the NI cDAQ-9174 chassis for data acquisition and the NI 9234 module for acquisition and synthesizing the data from accelerometers, and, on the other hand, the NL-602U-type GPS receiver for monitoring and recording the vehicle velocity.

The measurement of the accelerations was conducted for the circulation at constant speed, on a current line, in straight track. Registrations for the accelerations at the velocities of 117 and 137 km/h for sequences of 20 s at the sampling frequency of 2048 Hz were made. For instance, Figure 10 features the accelerations recorded by the two accelerometers for a measurement sequence at speed 137 km/h. The two accelerations are similar and the maximum value is about 4 g.

Figure 11 exhibits the spectra of the accelerations measured on the bogie frame for a measuring sequence at a velocity of 137 km/h, in the 1–200 Hz frequency range. The spectra of the accelerations show more peaks between 6.2 and 150 Hz, where the frequency peak at 6.2 Hz corresponds to the resonance frequency of the bogie bounce. For this interval, several local more peaks can be seen, in an arithmetic progression. The first peak corresponds to the frequency of 13.15 Hz, while the other peaks are located at the following frequencies: 26.25, 39.45, 52.45, 65.85, 78.65, 91.9, 105.3 and 118.1 Hz. The first peak comes from the wheel eccentricity, the second from its ovality and from the third to the ninth degree from the undulatory wear of the wheel rolling surface. Another peak can be seen at 17.15 Hz, which matches the wavelength of 2.2 m of the irregularities of the rail rolling surface, meaning a long-wave rail undulatory wear.

Further on, the RMS accelerations measured at velocities of 117 and 137 km/h, respectively, are introduced. To compare such results with the RMS accelerations derived from numerical simulations, the measured accelerations are bandpass filtered in the frequency interval that corresponds to the wavelengths of the track irregularities for 3–120 m and to the velocity. For instance,

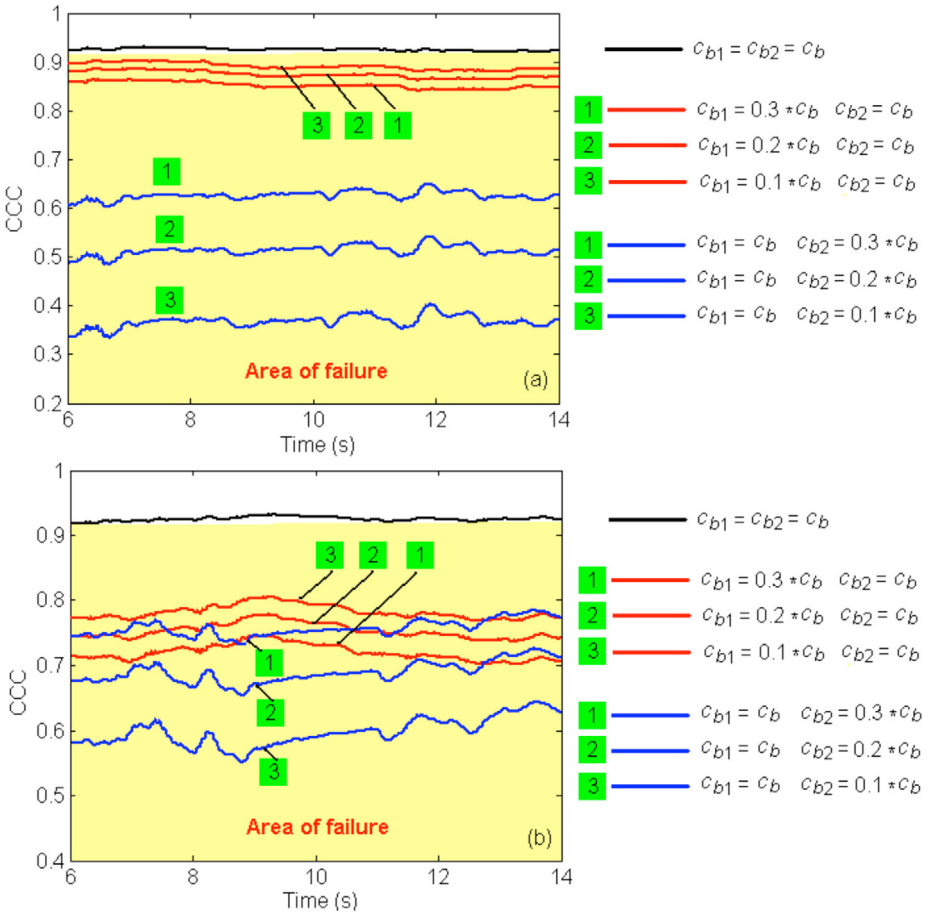

Fig. 8. The CCC of the bogie accelerations for different failure degrees of the damper: (a) at velocity of 117 km/h; (b) at velocity of 137 km/h.

Table 2. The average values of CCC for different failure degrees of the damper.

Damper condition	Failure degree	CCC	
		at $V = 117$ km/h	at $V = 137$ km/h
Normal	–	0.925	0.925
Defect damper in the suspension of the axle 1	70%	0.782	0.890
	80%	0.753	0.874
	90%	0.720	0.852
Defect damper in the suspension of the axle 2	70%	0.757	0.554
	80%	0.690	0.513
	90%	0.597	0.367

Figure 12 shows the spectra of the accelerations measured on a time sequence at a speed of 137 km/h, filtered in the 0.32–12.68 Hz frequency range.

Figure 13 shows the RMS accelerations for 25 measurement sequences at the constant speed of 117 km/h and the RMS accelerations derived from numerical simulations. The measured accelerations were bandpass filtered in the range frequency of 0.27–10.83 Hz. Each measurement sequence is described by a certain value of the RMS acceleration, the values are between 0.80 and 1.84 m/s^2, with an average value of 1.15 and 1.19 m/s^2. This interval also contains the value of the RMS acceleration from numerical simulations. This value is very close to the average value of the measured RMS accelerations. The difference between the RMS acceleration from numerical simulations and the average of the measured RMS accelerations does not exceed 10%.

Figure 14 features the RMS acceleration for 20 measurement sequences at the constant speed of 137 km/h and the RMS accelerations from numerical simulations. In this case, the measured accelerations were

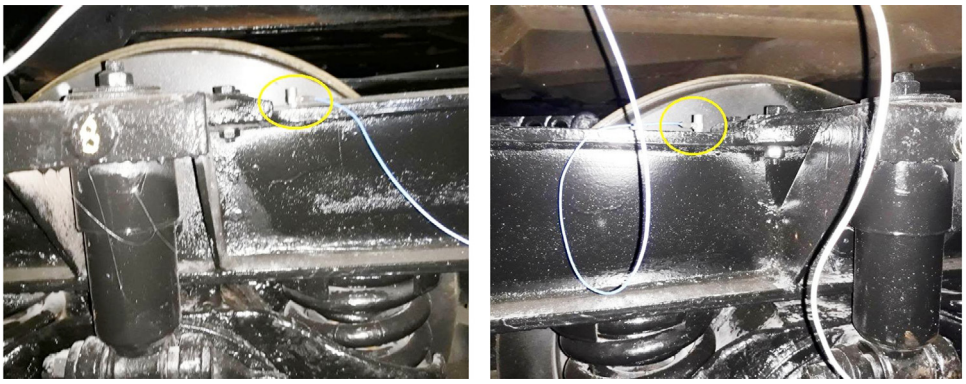

Fig. 9. Mounting accelerometers on the bogie frame.

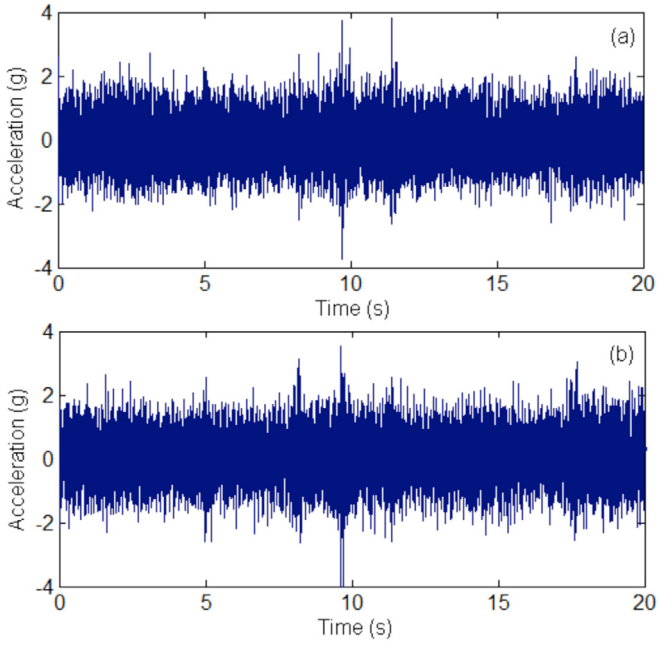

Fig. 10. Accelerations recorded on a measured sequence at speed 137 km/h: (a) on the bogie frame above axle 1; (b) on the bogie frame above axle 2.

bandpass filtered in the 0.31–12.68 Hz frequency range. The RMS accelerations measured on the bogie frame vary from 1.04 to 2.40 m/s^2 – above axle 1, with an average of 1.63 m/s^2, and from 1.03 to 2.49 m/s^2 – above axle 2, with an average of 1.75 m/s^2. Herein, the differences between the RMS acceleration from numerical simulations and the average values are higher than 10%, namely 18% – above axle 1; 14% – above axle 2.

3.2 Calculation of the cross-correlation of the measured accelerations

In this section, the results concerning the CCC of the accelerations measured on the bogie frame against the two axles calculated by the above method for measuring sequences of 20 s are herein introduced.

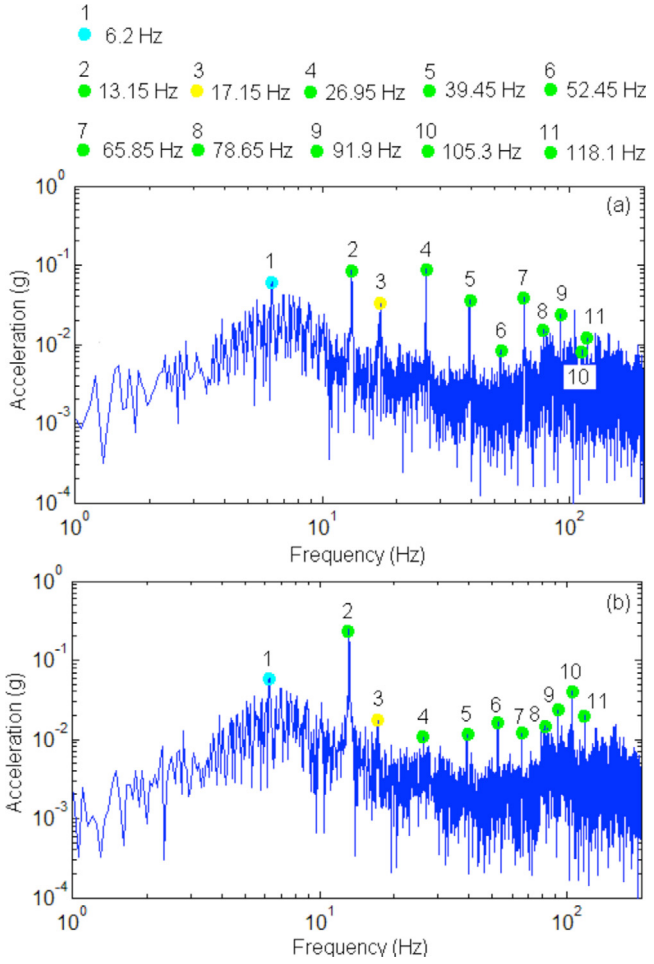

Fig. 11. Spectra of the acceleration measured at speed of 137 km/h: (a) on the bogie frame over axle 1; (b) on the bogie frame over axle 2.

Figure 15 shows the CCC of the accelerations for different measuring sequences at the velocity of 117 and 137 km/h in Figure 16. The CCC for two accelerations has the same characteristics as the ones above, irrespective of the measuring sequence. At the time moments $\tau = -0.06$ and $\tau = -0.08$ corresponding to the delay between the two accelerations, CCC has maximum values that are very

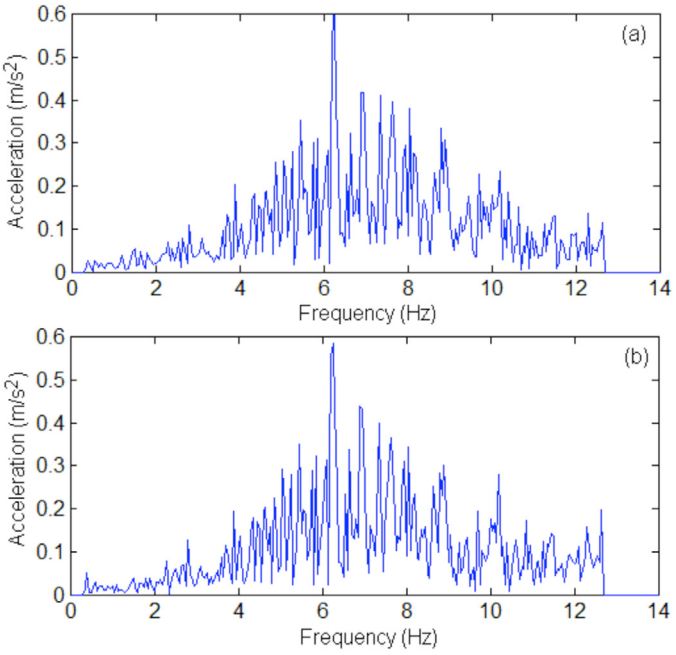

Fig. 12. Spectra of the acceleration measured at speed of 137 km/h, bandpass filtered in the range frequency of 0.32–12.68 Hz: (a) on the bogie frame above axle 1; (b) on the bogie frame above axle 2.

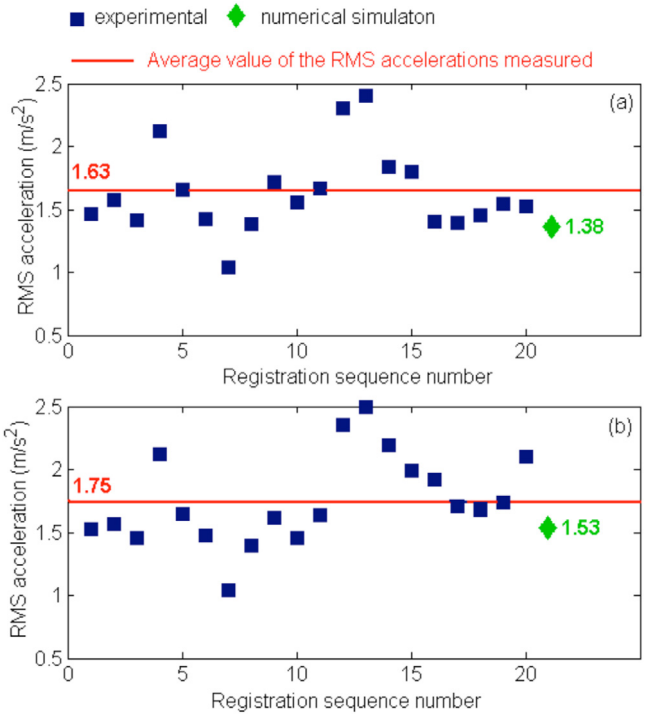

Fig. 14. The RMS accelerations at the speed of 137 km/h: (a) on the bogie frame above the axle 1; (b) on the bogie frame above the axle 2.

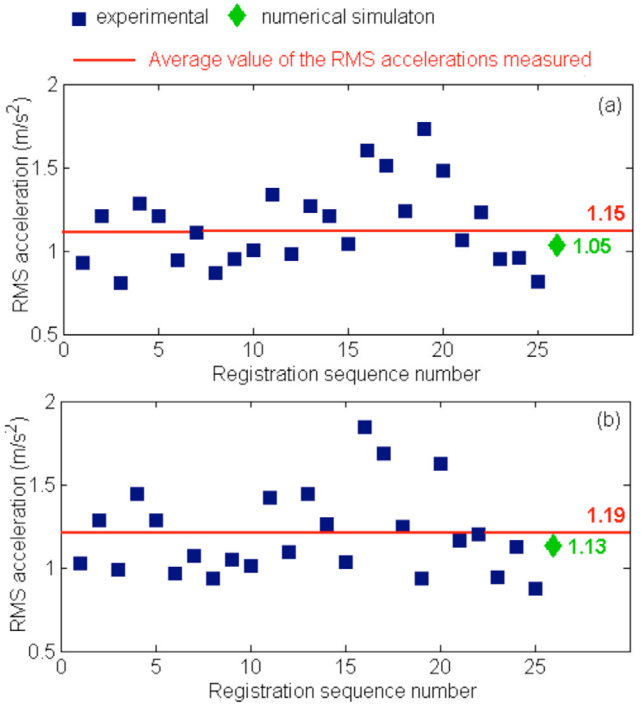

Fig. 13. The RMS accelerations at the speed of 117 km/h: (a) on the bogie frame above axle 1; (b) on the bogie frame above axle 2.

close to 1. This fact proves that there is a good correlation between the accelerations measured on the bogie frame against the axles.

Figure 17 shows the fact that values of the CCC of the accelerations for different measuring sequences are grouped in narrow intervals for the same velocity. At the speed of 117 km/h, CCC ranges from 0.85 to 0.96, while at 137 km/h, CCC is between 0.88 and 0.96.

4. Analysis of the results concerning the cross-correlation of the accelerations derived from numerical simulations and the cross-correlation of the measured accelerations

Figure 18 features the values of the CCC of the bogie frame accelerations for more measuring sequences at velocities of 117 and 137 km/h and the values of the CCC of the accelerations derived from the numerical simulations. The latter values are noticed to be in the central area of the dispersion interval of the values CCC of the measured accelerations. Moreover, as seen in Figure 19, the mean value of the CCC for the accelerations derived from numerical simulations at velocity of 117 km/h is very close to the average of the mean values of the measured accelerations, and they are practically equal at the velocity

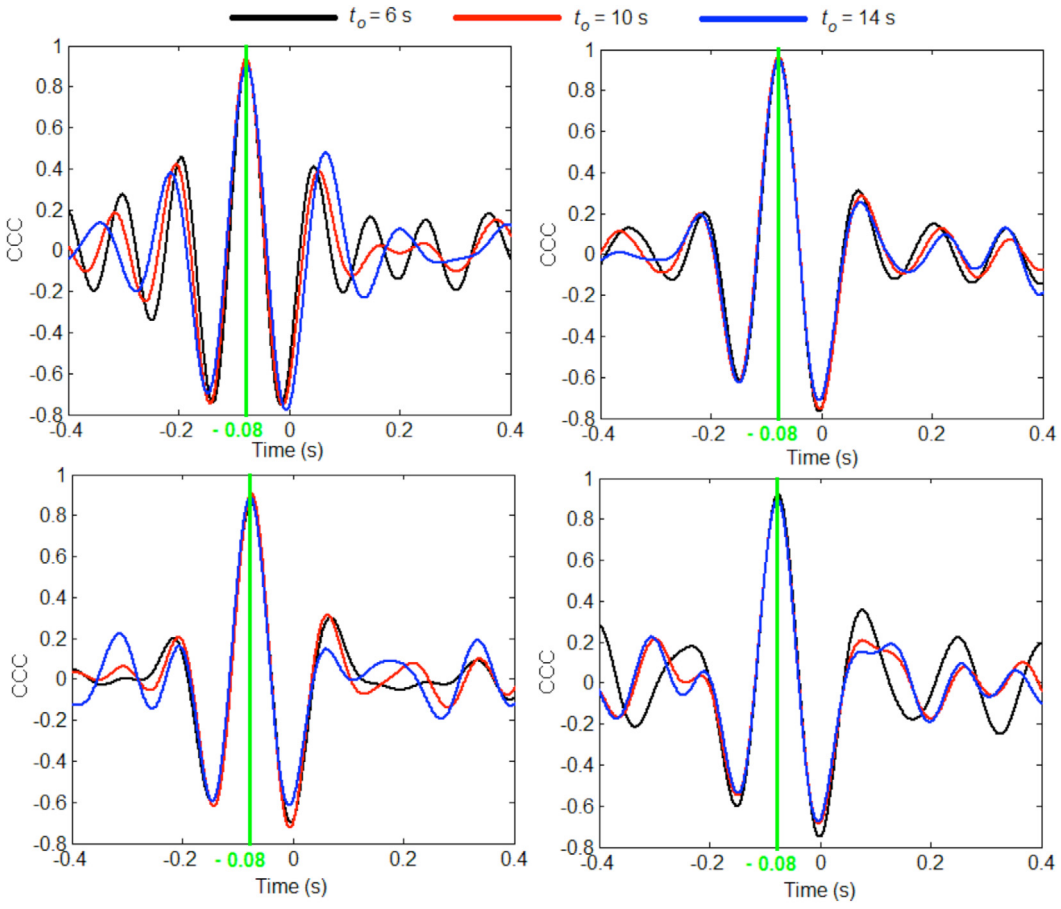

Fig. 15. The CCC of the accelerations measured at velocity of 117 km/h.

of 137 km/h. These results prove a good concordance between the results from theoretical model and the experiments.

Figure 18 shows the "area of failure" as the area that is limited in the superior part by the lowest value of CCC for the measured accelerations. The superior limit of the failure area depends, however, on velocity. For this case, a CCC lower than 0.85 indicates a defect in the damper at the velocity of 117 km/h. At the speed of 137 km/h, the failure in the damper can be visible for a CCC lower than 0.88.

5 Conclusions

The paper points out that the failure of a damper in the vertical primary suspension of the rail vehicles can be detected based on the change of the CCC of the accelerations measured on the bogie frame against the axles. The feasibility of the method is highlighted based on the results from applications of numerical simulations, where the failure of the damper is simulated by various degrees of reduction of the damping constant of the suspension corresponding to one of the wheels, compared with the reference value. The results herein show that the highest values of CCC occur when there is no damper defect, calculated at the time moment corresponding to the delay in the bogie response against the two axles. This fact shows a good correlation between the accelerations of the bogie calculated against the two axles. The CCC lowers when one of the damper fails and the higher the failure degree in the damper, the more significant reduction in the CCC.

The results concerning the CCC of the accelerations measured on a bogie in a passenger vehicle during circulation on a current line are in agreement with the results of the numerical simulations corresponding to the "no defect damper" situation. Practically, they show a good correlation between the measured accelerations. Moreover, the so-called "area of failure" is defined as the area that is limited in the superior part by the lowest value of CCC of the measured accelerations. The superior limit of the area of failure depends on velocity, yet the CCC values are very close to each other. In order not to count this fact an inconvenience for implementing the method of detecting the damper failure, based on the cross-correlation of the bogie accelerations, a limit value of failure can be set up so as to cover the operating velocities of the vehicle.

Acknowledgment. This work was supported by a grant from the Romanian National Authority for Science Research and Innovation, UEFISCDI, project number PN-III-P2-2.1-PED-2016-0212, within PNCDI III.

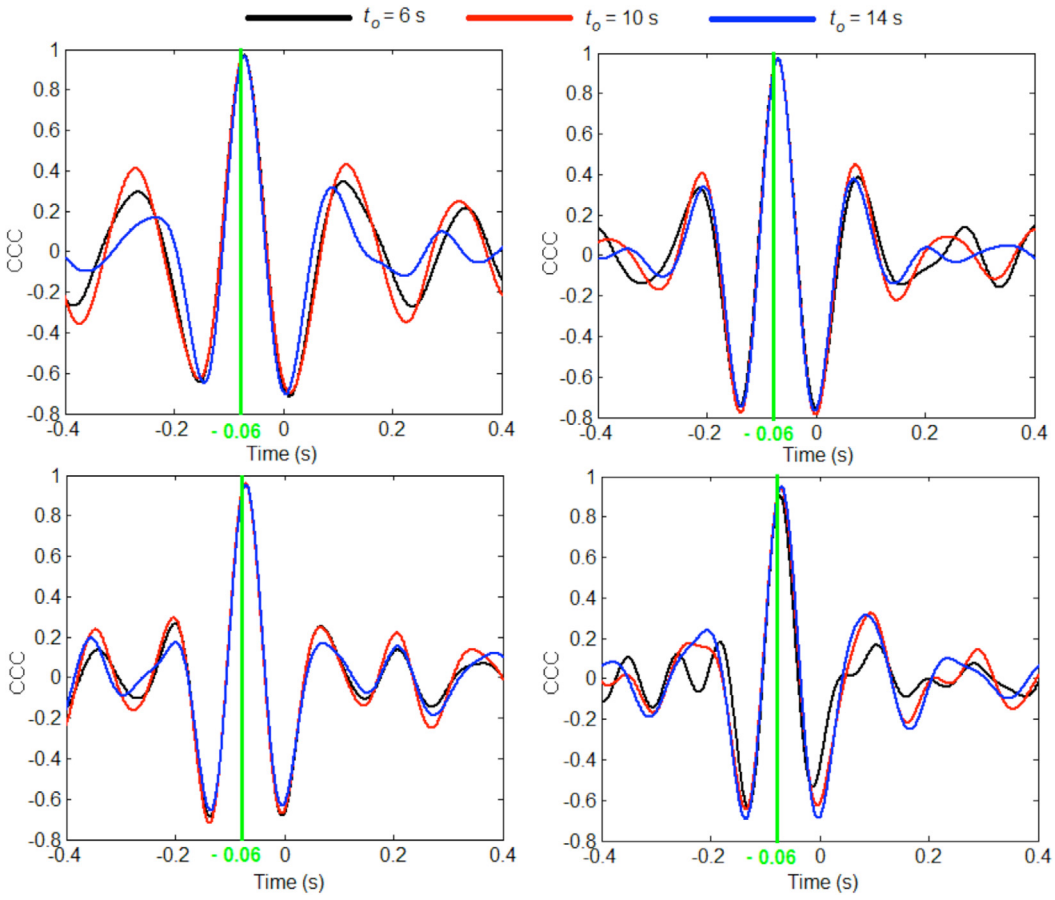

Fig. 16. The CCC of the accelerations measured at 137 km/h.

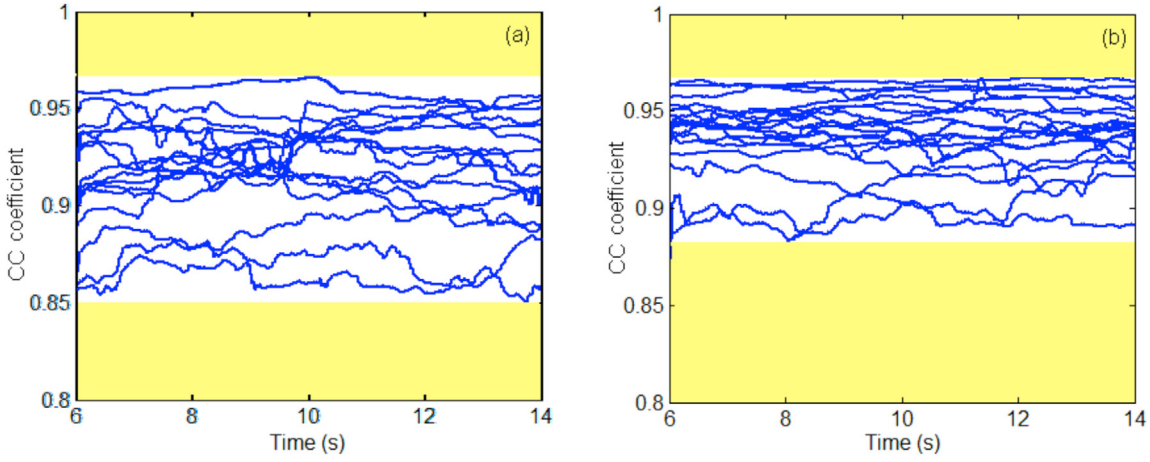

Fig. 17. The CCC of the measured accelerations at $\tau = -\ 2a_b/V$ for different measuring sequences: (a) $V = 117$ km/h; (b) $V = 137$ km/h.

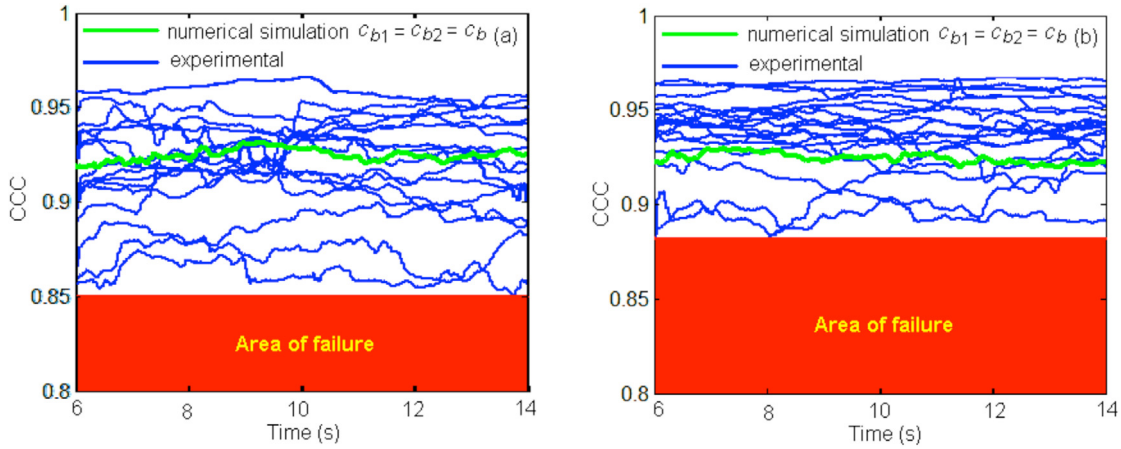

Fig. 18. Comparison between the CCC of the measured accelerations and the CCC of the accelerations from numerical simulations: (a) $V = 117$ km/h; (b) $V = 137$ km/h.

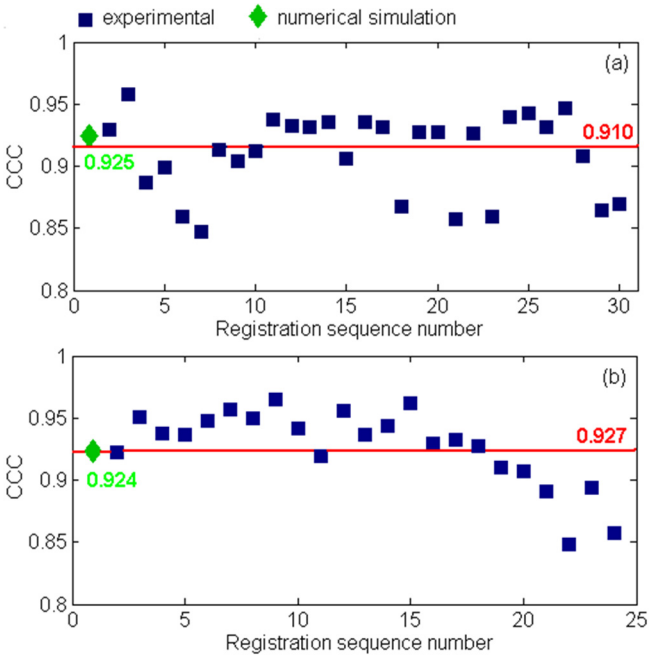

Fig. 19. The mean value of the CCC of the measured accelerations and of the CCC of the accelerations from numerical simulations: (a) $V = 117$ km/h; (b) $V = 137$ km/h.

References

[1] S. Kraft, C. Funfschilling, G. Puel, D. Aubry, Predictive maintenance by the identification of suspension parameters from online acceleration measurements, Proceedings of ISMA, 2010, pp. 3503–3518

[2] S. Bruni, R. Goodall, T.X. Mei, H. Tsunashima, Control and monitoring for railway vehicle dynamics, Veh. Syst. Dyn. 45 (2007) 743–779

[3] R.M. Goodall, C. Roberts, Concept and techniques for railway condition monitoring, Proceedings of the International Conference on Railway Condition Monitoring, 2006, pp. 90–95

[4] R.W. Ngigi, C. Pîslaru, A. Ball, F. Gu, Modern techniques for condition monitoring of railway vehicle dynamics, J. Phys. Conf. Ser. 364 (2012) 012016

[5] M. Dumitriu, Numerical analysis of the influence of lateral suspension parameters on the ride quality of railway vehicles, J. Theor. Appl. Mech. 54 (2016) 1231–1243

[6] M. Dumitriu, Influence of the suspension damping on ride comfort of passenger railway vehicles, UPB Sci. Bull. D Mech. Eng. 74 (2012) 75–90

[7] M. Dumitriu, Influence of the longitudinal and lateral suspension damping on the vibration behaviour in the railway vehicles, Arch. Mech. Eng. 62 (2015) 115–140

[8] M. Dumitriu, A parametric study on the influence of the nonlinear characteristics of the secondary suspension upon the vertical vibrations in the railway vehicles, UPB Sci. Bull. D Mech. Eng. 80 (2018) 125–140

[9] S. Alfi, S. Bionda, S. Bruni, L. Gasparetto, Condition monitoring of suspension components in railway bogies, Proceedings of the 5th IET Conference on Railway Condition Monitoring and Non-Destructive Testing, 2011, pp. 1–6

[10] P. Li, R. Goodall, P. Weston, C.S. Ling, C. Goodman, Estimation of railway vehicle suspension parameters for condition monitoring, Control Eng. Pract. 15 (2007) 43–55

[11] M. Jesussek, K. Ellermann, Fault detection and isolation for a railway vehicle by evaluating estimation residuals, Procedia IUTAM 13 (2015) 14–23

[12] M. Jesussek, K. Ellermann, Fault detection and isolation for a nonlinear railway vehicle suspension system, J. Vib. Eng. Technol. 3 (2015) 743–758

[13] J.S. Sakellariou, J.S. Konstantinos, A. Petsounis, S.D. Fassois, Vibration based fault diagnosis for railway vehicle suspensions via a functional model based method: a feasibility study, J. Mech. Sci. Technol. 29 (2015) 471–484

[14] M. Dumitriu, Influence of damping suspension on the vibration eigenmodes of railway vehicles, Mech. J. Fiability Durability 1 (2013) 109–115
[15] P.M. Frank, S.X. Ding, T. Marcu, Model-based fault diagnosis in technical processes, Trans. Inst. Meas. Control 22 (2000) 57–101
[16] P. Li, R. Goodall, Model-based condition monitoring for railway vehicle systems, Proceedings of the UKACC International Conference on Control, University of Bath, UK, September 2004
[17] H. Tsunashima, Y. Hayashi, H. Mori, Y. Marumo, Condition monitoring and fault detection of railway vehicle suspension using multiple-model approach, Proceedings of the 17th World Congress, the International Federation of Automatic Control, Seoul, Korea, July 6–11, 2008, pp. 584–589
[18] H. Tsunashima, H. Mori, Condition monitoring of railway vehicle suspension using adaptive multiple model approach, Proceedings of the International Conference on Control, Automation and Systems, Gyeonggi-do, Korea, 2010, pp. 584–589
[19] T. Oba, K. Yamada, N. Okada, K. Tanifuji, Condition monitoring for Shinkansen bogies based on vibration analysis, J. Mech. Syst. Transport. Logistics 2 (2009) 133–144
[20] X. Wei, L. Jia, H. Liu, A comparative study on fault detection methods of rail vehicle suspension systems based on acceleration measurements, Veh. Syst. Dyn. 51 (2013) 700–720
[21] M. Dumitriu, Numerical synthesis of the track alignment and applications. Part I: the synthesis method, Transp. Probl. 11 (2016) 19–28
[22] C 116, Interaction between vehicles and track, RP 1, Power spectral density of track irregularities, Part 1: definitions, conventions and available data, Utrecht, 1971
[23] UIC 518 Leaflet, Testing and approval of railway vehicles from the point of view of their dynamic behaviour – safety – track fatigue – running behaviour, 2009
[24] M. Dumitriu, Analysis of the dynamic response in the railway vehicles to the track vertical irregularities. Part II: the numerical analysis, J. Eng. Sci. Technol. Rev. 8 (2015) 32–39

Cite this article as: M. Dumitriu, Fault detection of damper in railway vehicle suspension based on the cross-correlation analysis of bogie accelerations, Mechanics & Industry **20**, 102 (2019)